Article

The Fundamental Neurobiological Mechanism of the Oxidative Stress-Related Deamidation Reaction in the 4E-BP2 Protein

Davis Joseph *

Posted Date: 1 November 2024

doi: 10.20944/preprints202410.2493.v2

Keywords: 4E-BP2; Deamidation; Alzheimer's; oxidative stress; neurodegeneration

 doi:10.20944/preprints202410.2493.v2

Article

The Fundamental Neurobiological Mechanism of the Oxidative Stress-Related Deamidation Reaction in the 4E-BP2 Protein

Davis Joseph [1,2,*]

[1] McGill University
[2] FLOGEN Technologies Inc
* Correspondence: davisandrejoseph@gmail.com or djoseph@flogen.com

Abstract: 4E-BP2 deamidation significantly alters protein production in the brain and nervous system. It maintains the balance of protein production required for a healthy nervous system. Any imbalance in protein production in the brain and nervous system causes all neurodegenerative diseases. Discovering what causes 4E-BP2 deamidation only in neurons will make it possible to control this balance of protein production and cure neurodegenerative diseases such as memory loss, Alzheimer's, and Parkinson's. Alzheimer's disease is caused by the absence of 4E-BP2 protein in the brain's neurons. This protein undergoes deamidation spontaneously only in the neurons and, in this way, controls the production of proteins in the neurons. This, in turn, determines whether or not Alzheimer's and Parkinson's disease start or progress. The purpose of this work is to discover the neurobiological mechanism that causes the deamidation reaction in the 4E-BP2 protein by performing immunoblotting in the retinal ganglia, the optic nerve, the dorsal root ganglia, the sciatic nerve, and the whole brain, extracted via dissection from 2-month-old, Wild-type male mice. The results showed that deamidation mainly occurs in the axons or axon-enriched regions of the optic nerve, the whole brain, and the sciatic nerve, confirming conclusively that axons are the critical factors behind the neurobiological mechanism of 4E-BP2 protein deamidation. The results confirm that they are also the reason why 4E-BP2 deamidation occurs only in neural tissue.

Keywords: 4E-BP2; deamidation; Alzheimer's; oxidative stress; neurodegeneration

1. Introduction

In 1976 the eIF4E (eukaryotic translation initiation factor) was discovered [1]. This protein binds to the m7GpppN cap structure of the mRNA and initiates the translation of proteins by directing ribosomes to said cap structure and forming the eIF4F complex [1]. In 1994, 4E-BP proteins were discovered [2]. These proteins bind to the eIF4E protein, inhibit the binding of eIF4G to eIF4E, and therefore prevent the formation of the eIF4F complex and the overall translation of proteins [2]. In 1999 and 2005, deamidation was associated with oxidative stress [3,4]. Deamidation was later characterized as a recycling mechanism for proteins damaged by oxidative stress [5]. In 2007, it was discovered that 4E-BP2, which is the dominant paralog of 4E-BPs in brain tissue, undergoes deamidation, the conversion of an asparagine to an aspartic acid, at the N99 and N102 amino-acids only when found in the neurons. The deamidation of 4E-BP2 decreases the affinity for eIF4E and increases it for the raptor component of mTORC1. Deamidation occurs 18 days after birth in the mouse brain. Before 18 days, the protein is phosphorylated instead of deamidated in this region. Deamidation was also found to increase with increasing pH [6]. Deamidation occurs in Asparagines 99 and 102 in 4E-BP2 18 days after birth [6]. Deamidation occurrence is observed in western blots by the appearance of three bands on the blot using 4E-BP2 antibodies. The bottom band represents un-deamidated 4E-BP2, the middle band represents 4E-BP2 where either Asn 99 or Asn 102 is

 doi:10.20944/preprints202410.2493.v2

deamidated, and the top band represents 4E-BP2 where both asparagines are deamidated [6]. In 2017, it was claimed that 4E-BP2 deamidation was also found in muscle cells [7].

However, since 2007, when it was discovered that 4E-BP2 undergoes deamidation, there has been no credible explanation for why deamidation of 4E-BP2 occurs only in neural tissue. Several theories were previously postulated. One was that higher brain pH than the rest of the body leads to deamidation. However, other publications [8] have shown that the brain's pH is lower on average than the rest of the body. The average pH in the brain is 7.05, and the average pH of the body falls within the range of 7.35-7.458 [8]. Another postulated theory was that deamidation was caused by a lower turnover rate of proteins in non-dividing cells such as neurons [7]. However, the same author looked at deamidation in heart muscle cells, which are also non-dividing, just like neurons, and found the deamidation rate in heart muscle cells insignificant [7].

The question is: What is the real cause of 4E-BP2 deamidation in the brain? Discovering the fundamental neurobiological mechanism behind 4E-BP2 deamidation is of crucial and seminal importance for the following reasons:

1. It will lead one step closer to understanding this fundamental mechanism, which is critical to the inner machinations of human consciousness because 4E-BP2 deamidation significantly changes the brain's translation (protein production) rates [6]. 4E-BP2 is also directly linked to the fundamental biological mechanism of memory [9].
2. It will be crucial to developing therapeutics against Alzheimer's and Sclerosis since:
    - The absence of deamidated 4E-BP2 in the brain leads to the development of Alzheimer's disease [10].
    - Deamidation is related to aggregation and amyloid plaque formation, which is the root cause of memory loss in Alzheimer's and many other neurodegenerative diseases. Deamidation accelerates amyloid formation and alters amylin fiber structure [11].
3. It is indispensable to the survival of the mammalian brain because 4E-BP2 deamidation has been conserved in all mammals for 90 million years. Therefore, this function is crucial to all mammalian brains [12].

Therefore, the purpose of this paper is to (1) describe a newly developed fundamental theory of the deamidation mechanism that demystifies 4E-BP2 deamidation as a process that occurs only in neurons, something that could not be done in 17 years and (2) validate it experimentally in both the central nervous system (CNS) and the peripheral nervous system (PNS) by performing western blots of 4E-BP2 on the optic nerve, the sciatic nerve, the whole brain, the retinal ganglia and the dorsal root ganglia of 2-month-old male Wild-type mouse models.

In summary, since 4E-BP2 controls protein production in the brain, it plays a crucial role in the progression of neurodegenerative diseases. 4E-BP2 when undergoing a chemical reaction called deamidation, which is traditionally linked to oxidative stress, can no longer bind the eIF4E protein and this fundamentally changes translation in the nervous system, which is why discovering the cause of 4E-BP2 deamidation in the brain is of utmost importance.

My hypothesis to be proven was the following:

4E-BP2 deamidation happens only in neurons because of the axons and their unique properties.

2. Results

2.1. Experiments in the Whole Brain, the Optic Nerve and the Retina of the Central Nervous System (CNS)

The first goal of the first experiment was to compare 4E-BP2 deamidation in the two parts of the neurons of the brain:

a) The axons

b) The cell bodies (soma)

The first tests were performed on the central nervous system (CNS), because the protein in question, 4E-BP2, is the most prevalent 4E-BP protein in the brain [6]. One specific nerve of the CNS needed to be isolated to study the prevalence of 4E-BP2 deamidation in the axon compared to its respective ganglia (soma). It would reflect where 4E-BP2 deamidation is most prevalent in myelinated neurons, the dominant type of neurons in the CNS [13]. The optic nerve was chosen to be

 doi:10.20944/preprints202410.2493.v2

studied in this paper because the optic nerve is a large nerve of the mouse CNS, which is isolatable via dissection. The retina was also dissected for comparison because it is where the optic nerve axons' soma (retinal ganglia) are located. The optic nerve and the retina are extensions of the brain because, during embryonic development, they arise from the diencephalon, a brain division [14–16]. The results are shown in Figure 1.

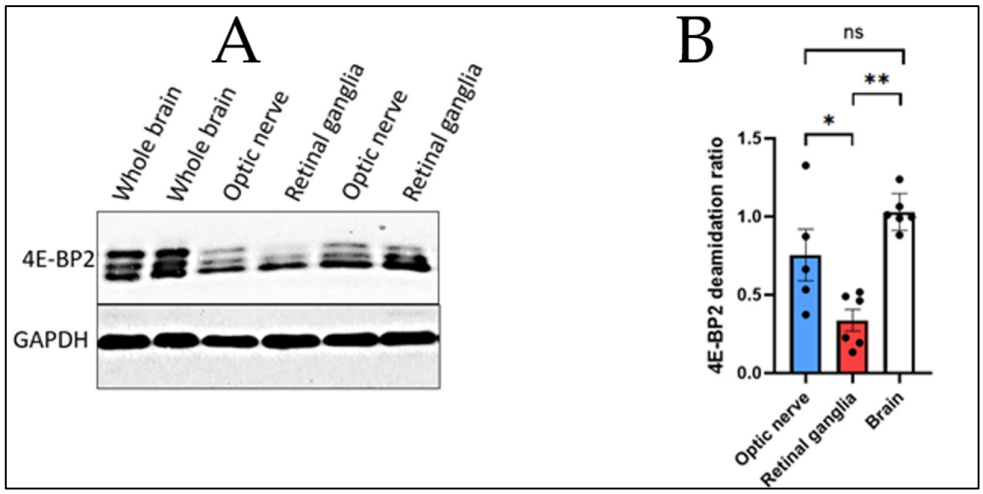

Figure 1. 4E-BP2 Western blot of the whole brain, the optic nerve and the retinal ganglia from 2-month-old WT mice, using GAPDH as the control. (A) Immunoblotting data; (B) ANOVA statistical test comparing the deamidation ratios of the three organs studied using the Bonferroni-Holm procedure.

This was the first time that the optic nerve or the retina was dissected to detect 4E-BP2 deamidation.

The second goal of the first experiment was to compare 4E-BP2 deamidation in the whole brain (a mixture of axons and cell bodies) with the individually isolated axons in the optic nerve and cell bodies in the retina.

This comparison sheds light on where precisely 4E-BP2 deamidation originates.

The deamidation ratio was calculated for each region studied to accurately compare the level of deamidation in the axon-enriched brain and optic nerve with the cell body-enriched retinal ganglia.

The calculations are the following:

1. The optic nerve was found to have a deamidation ratio of 0.75388 based on five mice samples (N = 5)
2. The retinal ganglia were found to have a deamidation ratio of 0.3365 based on six mice samples (N = 6).
3. The axon-enriched whole brain was found to have a deamidation ratio of 1.030184 based on six mice samples (N = 6)

As seen in previous literature [17], the Bonferroni-Holm method after an ANOVA statistical test, chosen for this experiment, proves critical when analysing the three sample regions (see materials and methods section).

As a result of these calculations, the findings from Figure 1 are the following:

1. 4E-BP2 deamidation in the optic nerve axons is significantly higher than in the soma cell body-enriched retinal ganglia.
2. 4E-BP2 deamidation in the optic nerve axons shows no significant difference compared to deamidation in the axon-enriched whole brain.
3. 4E-BP2 deamidation in the cell body-enriched retinal ganglia is significantly lower when compared to deamidation in the axon-enriched whole brain.

Based on these findings, the following conclusion can be drawn from Figure 1:

Deamidation in the central nervous system comes from the axons.

 doi:10.20944/preprints202410.2493.v2

2.2. Experiments in the Sciatic Nerve and the Dorsal Root Ganglia (DRG) of the Peripheral Nervous System (PNS)

The goal of the second experiment was to compare 4E-BP2 deamidation in the two parts of the neurons of the periphery of the body:

a) The axons

b) The cell bodies (soma)

The tests in the PNS were performed to validate if 4E-BP2 deamidation is also axon-specific in this particular system, where nerves are far away from the brain. Like the CNS, one specific nerve of the PNS needed to be isolated to accurately study the prevalence of 4E-BP2 deamidation in the axon compared to its respective ganglia (soma).

The sciatic nerve was chosen to be studied in this paper because it is the largest and longest nerve of the mouse PNS, which is isolatable via dissection [18]. The results are shown in Figure 2.

This was the first time the sciatic nerve was dissected to detect 4E-BP2 deamidation.

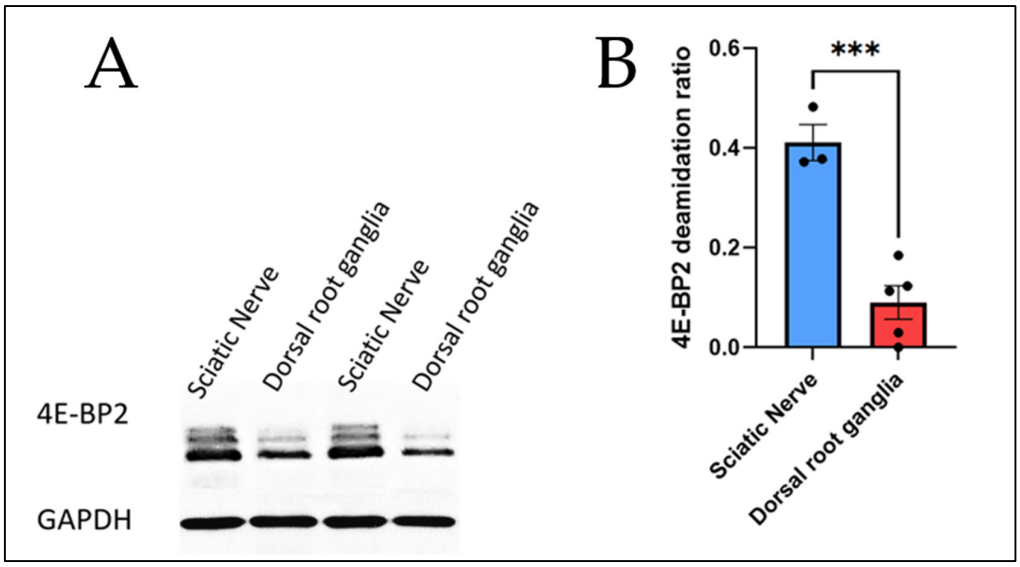

Figure 2. 4E-BP2 western blot of the sciatic nerve and the dorsal root ganglia from 2-month-old WT mice and GAPDH as the control. (A) Immunoblotting data; (B) T-test comparing the deamidation ratios of the two organs studied.

The calculations of the deamidation ratios (as described previously) are the following:

1. The sciatic nerve has a deamidation ratio of 0.411231 based on three mice samples (N = 3)
2. The dorsal root ganglia have a deamidation ratio of 0.090206 based on five mice samples (N = 5).

Based on these calculations from a statistical t-test, Figure 2 shows that 4E-BP2 deamidation in the sciatic nerve axons is significantly higher than deamidation in the soma cell body-enriched dorsal root ganglia.

Based on these findings, the following conclusion can be drawn from Figure 2:

4E-BP2 deamidation in the PNS comes from the axons, and the findings in the PNS corroborate the findings the CNS.

An important observation is noted when comparing Figures 1 and 2: the longer the axon, the more significant the average difference in deamidation. The average length of the optic nerve in the mouse ranges from 5 mm [19], and the average length of the mouse sciatic nerve ranges from 22.6 +/- 1.62 mm [20]. When looking at the difference in deamidation of 4E-BP2 in my results, I find that deamidation in the axon tissue of the optic nerve, which is fully myelinated according to previous studies [21], is 2.24 times more significant than in the retinal ganglia, based on my results in Figure 1. However, when comparing 4E-BP2 deamidation in the sciatic nerve and the dorsal root ganglia, I find that sciatic nerve deamidation is 4.59 times higher in the axon based on my results.

 doi:10.20944/preprints202410.2493.v2

From this observation, I conclude that a significant increase in the neuron's length more than doubles the difference in 4E-BP2 deamidation ratios.

In Figure 3, the rates of deamidation were compared between the sciatic nerve, where axons are mostly unmyelinated [22] (not isolated), and the whole brain, where axons are mostly myelinated [23,24] (isolated), to determine the effect of myelination on deamidation. Myelin plays a crucial role in multiple neurodegenerative diseases, such as multiple sclerosis [25].

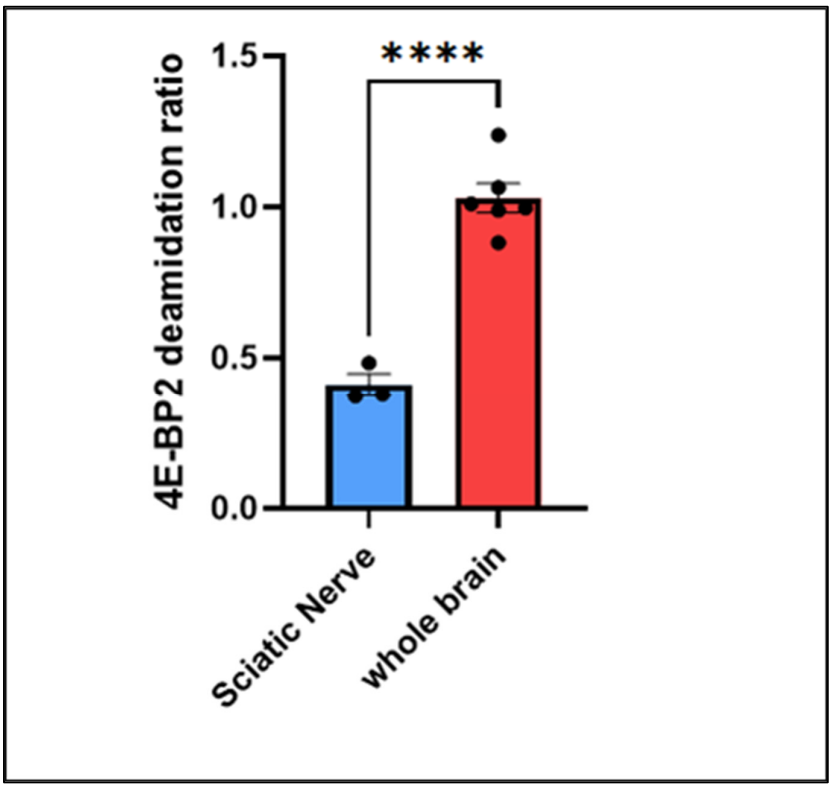

Figure 3. T test comparison between the deamidation ratios of the whole brain and the sciatic nerve.

Based on the comparison, the following conclusion can be drawn from Figure 3:

Deamidated 4E-BP2 is more enriched in the myelinated axons of the whole brain compared to the mostly unmyelinated axons of the sciatic nerve.

Establishment of the Theory of the Neurobiological Deamidation Mechanism

3. Discussion

Based on the above experimental results and their analysis, the following conclusions can be drawn:

1. Deamidation in the central nervous system comes from the axons.
2. Deamidation in the peripheral nervous system comes from the axons.
3. Deamidated 4E-BP2 is more enriched in the myelinated axons of the whole brain than in the sciatic nerve's mostly unmyelinated axons.

Each of these conclusions are discussed below:

3.1. Half-Life Length: The Cause of 4E-BP2 Deamidation Being Neuron-Specific

My literature analysis reveals that deamidation is a spontaneous reaction, and no enzyme is necessary for deamidation [6]. Each asparagine in proteins is found to have a deamidation half-life, after which more than 50% of said asparagines are converted into aspartic acids [26]. Also, it has been

 doi:10.20944/preprints202410.2493.v2

determined [26,27] that deamidation depends on the exposure of the asparagine or glutamine to the solvent, which is determined by the protein structure and the flanking amino acids. Based on the above literature, I concluded that the smaller the amino acids flanking the specified asparagine in 4E-BP2 are, the more this asparagine is exposed to the solvent. Also, the more the asparagine is exposed to the surrounding solvent, the shorter the half-life of the asparagine will be before it is converted into an aspartic acid. For instance, it has been found, based on Robinson's deamidation algorithms, that Asparagine 21 in the ESNGP amino acid sequence of the SOD1 protein has a half-life of 71 days. In contrast, Asn 53 in the GDNTA amino acid sequence of the same protein, less exposed to the solvent, has a half-life of 17127 days [26–28]. I concluded that the half-life of Asparagine 99 and 102 in the NNLNNLNNH amino acid sequence of 4E-BP2 to be reached 18 days after birth in neurons because this is consistently the amount of time required for deamidation to be significantly observed [6].

Since the NNLNNLNNH amino-acid sequence has no structure and this principle is identical in all 4E-BP2 proteins regardless of where it is found in the body [29], different exposures to the solvent cannot be the cause of 4E-BP2 deamidation being specific to neural tissue, the exposure to the solvent being identical everywhere in the body. Therefore, based on my analysis of the literature above, I concluded that deamidation only occurs in 4E-BP2 found in neural tissue because the protein half-life of 4E-BP2 is longer than the deamidation half-life of asparagines 99 and 102 only in neural tissue, allowing deamidation to occur in 4E-BP2 in this specific type of tissue in the body.

3.2. Axons: The Cause of the Increase of 4E-BP2 half-Life in Neurons

My literature analysis reveals that the protein half-life of proteins other than 4E-BP2 is significantly longer in axons. For instance, SOD1 proteins in the axons of the motor neurons of the spinal cord undergoing axonal transport had a protein half-life of over one year [30]. In contrast, the SOD1 proteins found in kidney cells had a half-life of only 100 hours [31].

Previous studies have shown that 4E-BP proteins have a half-life of only 20 hours outside of neurons, such as in pancreatic beta cells [32]. This proves as I concluded previously, that 4E-BP proteins in areas outside neurons have half-lives that are far too low to reach the 18-day threshold required for deamidation in Asn 99 and Asn 102. Also, 4E-BP2 proteins in neurons were found to have a significantly higher half-life than 4E-BP2 proteins in kidney cells [33].

My experimental conclusions 1 and 2 confirmed that deamidation occurs specifically in axons in the central and peripheral nervous systems.

Therefore, based on my experimental results, I concluded that 4E-BP2 deamidation happens specifically in the axon, because axons significantly increase protein half-life.

3.3. The Proteasome-Poor Environment in Axons- the Cause of the Increase of 4E-BP2 Half-Life

My literature critical analysis reveals that proteasome-poor environments such as erythrocytes have significantly longer protein half-lives [34]. Axons are also proteasome-poor compared to the soma due to ribosome biogenesis mainly being done in the soma [35].

Proteasomal activity is higher in neurons without myelin [25].

My experimental conclusion 3 confirmed that deamidated 4E-BP2 is more enriched in the myelinated axons (fewer proteasomes) of the whole brain than the mostly unmyelinated axons (more proteasome) of the sciatic nerve.

I conclude that the proteasome-poor environment in the axons is what makes 4E-BP2's half-life longer and deamidation thus possible.

3.4. Establishment of the Theory and Principle Behind 4E-BP2 Deamidation Based on These Findings

These three experimental conclusions comprise the Davis Joseph principle of the deamidation mechanism. It was developed over two weeks, starting on August 31, 2023, and finalized on September 13th, 2023, when I was 23 years old.

This principle can be concisely summarized as follows:

 doi:10.20944/preprints202410.2493.v2

Due to their proteasome-poor environment (the axonal cytoplasm), Axons increase the protein half-life, which becomes more significant than the deamidation half-life of asparagines, creating neuron-specific deamidation. The biological clock is now observed.

This fundamental principle is of tremendous importance because, as stated above, the neural tissue-specific deamidation process has been conserved in all mammals for 90 million years. Given 4E-BP2 and deamidation's role in the progression of the disease, the principle opens the way to multiple treatments for neurodegenerative diseases.

This principle, by tying 4E-BP2 deamidation to the proteasome-poor nature of the axonal cytoplasm, also opens the door to monumental research on possible treatments for Parkinson's. The first sign of Parkinson's progression is the degradation of motor axons, which is tied to a change in protein production [36].

The results of this paper are seminal because by proving that 4E-BP2 deamidation is found mainly in the axons, they explain why deamidation of 4E-BP2 occurs in neurons and why 4E-BP2 deamidation is also detected in muscles. As observed in a previous publication [37], each muscle cell is associated with one neuromuscular junction (NMJ), which contains a motor axon terminal. Considering this literature information, my theory explains that deamidation was found in muscles previously not because of the muscle cell itself but because of the motor axon terminal attached to the NMJ of each muscle fiber. My conclusion that the NMJ causes 4E-BP2 deamidation in the muscles is supported by previous literature that shows that the concentration of NMJ axon terminals is immense in the muscles, for example, in the bicep, where 172 000 to 400 000 muscle fibers are located. Each has its corresponding NMJ axon terminal [38,39]. My results in Figure 2 demonstrate that the sciatic nerve and its axon terminals, which, according to previous literature [40], are connected to muscle fibers by numerous NMJs, are where 4E-BP2 deamidation is produced.

Thus, my experimental and theoretical conclusions are corroborated by 4E-BP2 deamidation being previously detected in skeletal muscles [7], because skeletal muscles have a very high density of axon terminals found in the neuromuscular junctions [38].

Also, contrary to a previous literature study where the conclusion was that 4E-BP2 deamidation came from neurons and muscle cells [7], my work shows that the deamidation of 4E-BP2 found in muscles is coming from the axon terminal linked to the muscle fibers via the NMJ. The previous study used Synaptophysin antibody experiments to study the presence of synapses (axon terminals) in muscle cells. The study claimed that no synapses in the muscles were found after dissection. However, the method used was incorrect because the muscles were not permeabilized with either triton X-100 or a Cd2+ in a Ca2+-free medium before applying the synaptophysin antibody, as specified in the literature [41]. Based on the latter, without the permeabilization step, the axon terminal in the NMJ cannot be detected.

This work also showed that, despite the vast difference in tissue composition, location, and function between the optic nerve and the sciatic nerve, the same deamidation process is observed in both organs, as shown in Figures 1 and 2. As can be seen in these figures, although the optic nerve is entirely myelinated [21], whereas the sciatic nerve is a mixed neuron [42–44] containing both unmyelinated and myelinated axons, deamidation of Asn 99 and Asn 102 of the NNLNNLNNH amino-acid sequence in 4E-BP2 is mainly found in the 4E-BP2 proteins located in the axons. This finding validates this work's principle that deamidation is tissue-specific to neurons due to axons and their proteasome-poor environment.

There may be little deamidation in the ganglia dissected, but this is most likely due to the dissection process, which always leaves a bit of the axon at the root of the soma and the rest of the ganglia. The key here is that the retinal ganglia sample is cell body enriched, whereas the axon samples are pure. A significant difference in deamidation was thus seen when comparing pure axon samples with cell body-enriched samples, and 4E-BP2 deamidation was found to occur mainly in the axons.

The results from this study confirm that the nature of the axonal cytoplasm causes oxidation in translational control proteins. This means that axons may also cause oxidative stress and may also be

 doi:10.20944/preprints202410.2493.v2

the precursors of oxidative stress within the nervous system. This paves the way for seminal research into oxidative stress-related drug development against neurodegeneration.

To explain the procedure of the chemistry behind 4E-BP2 deamidation, I invented an organic chemistry flow sheet consisting of 5 intermediary molecules, as seen in Figure 4. In this figure, the reaction starts spontaneously at the level of the asparagine. During this spontaneous reaction, the secondary amide's nitrogen attacks the primary amide's carbonyl (step 1). This creates a cycle of atoms in intermediary 1. At the level of intermediary 1, the primary amine leaves the molecule (step 2), a process known as nucleophilic substitution that creates intermediary 2. At the level of intermediary 2, the deprotonation process occurs at the tertiary nitrogen (step 3), creating a succinimide molecule. At the level of succinimide, amide hydrolysis occurs (step 4), which produces intermediary 4. At the level of intermediary 4, the bond between the nitrogen and the carbon inside the succinimide ring is severed (step 5), which produces intermediary 5. At the level of intermediary 5, an intramolecular deprotonation (step 6) produces the aspartate under basic conditions, which is the last step of the reaction.

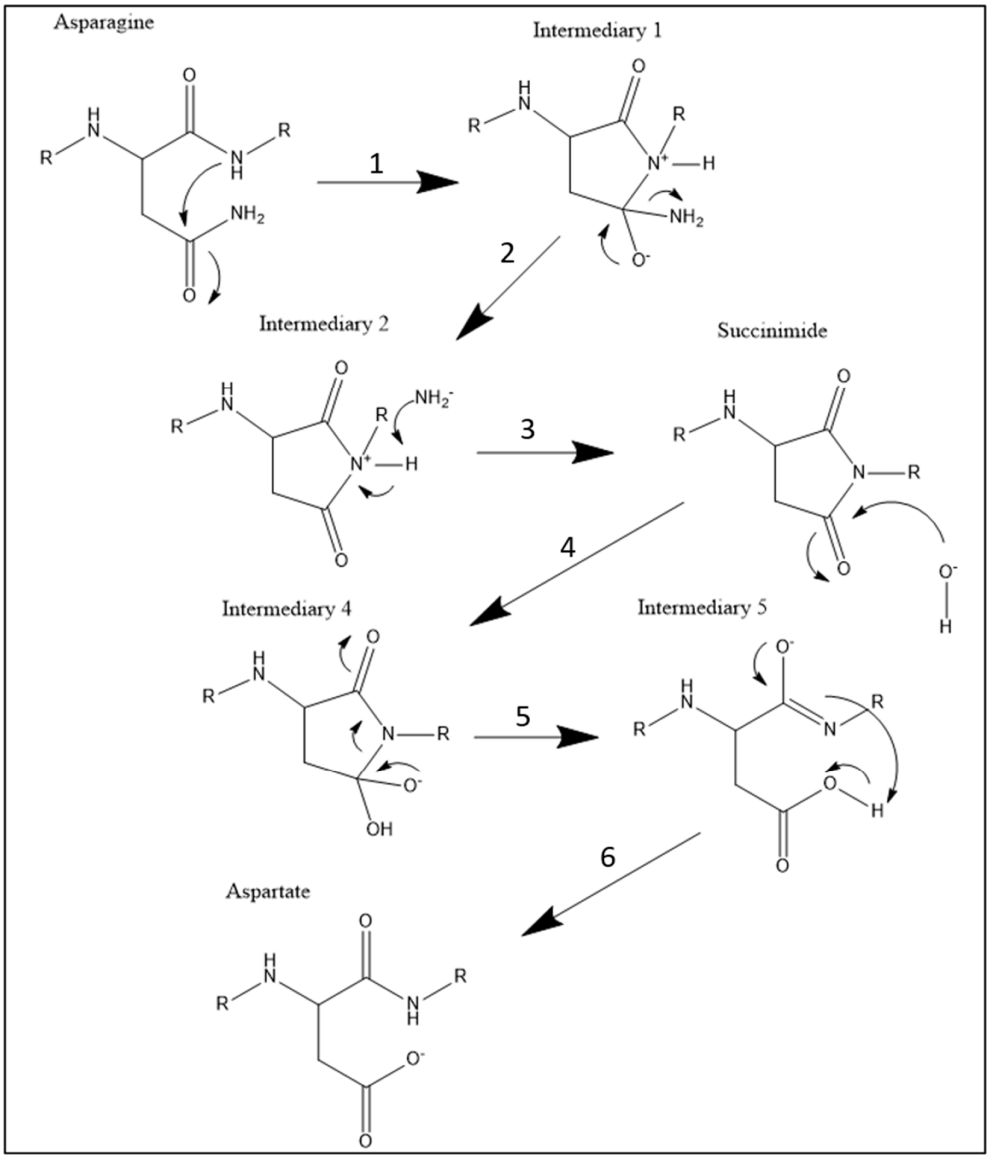

Figure 4. 6-step Chemical reaction of deamidation occurring in 4E-BP2 at positions N99 and N102.

 doi:10.20944/preprints202410.2493.v2

4. Materials and Methods

4.1. The Joseph Ratio (Statistical Analysis)

the intensity of the bottom band of 4E-BP2 represents the amount of non-deamidated 4E-BP2. In contrast, the intensity of the top band represents the amount of fully deamidated 4E-BP2 (deamidation having occurred in both Asn 99 and Asn 102). The Joseph ratio is the deamidation ratio I created. It is the amount of deamidated 4E-BP2 (the top band) divided by the amount of non-deamidated 4E-BP2 (the bottom band).

4.2. Statistical Analysis

The calculation results were obtained using the Bonferroni-Holm method after an ANOVA statistical test between the three sample regions. The Bonferroni correction and the Bonferroni-Holm method are done to avoid a type 1 statistical error, misinterpreting the data and concluding that there was a statistical difference when there was no difference [17].

4.2. Animal Tissue Sample Collection

The project identification code is MCGL-5205. The date of approval was August 30, 2023, by the McGill Animal Care committee. The mouse strain used is C57BL/6 (Controls WT in house).

I invented my own method of dissecting the optic nerve and the retina, without relying on previous literature. The method consists of euthanizing the mouse in a carbon dioxide chamber, followed by head decapitation. I proceeded by peeling off the mouse skin and then the skull. I also lifted the whole brain up from the base of the skull in order to expose the chiasma. Using a micro tweezer, I cut right between the chiasma and its connection to the diencephalon. I then proceeded the cut both connections between the optic nerve and the mouse retina.

After isolating the optic nerve, I then placed the mouse eyes on Wattman paper in order to keep them in place and isolated the retina using a scalpel.

I also invented my own unique way of dissecting the sciatic nerve without relying on previous literature. by severing the mouse leg using large scissors, peeling off the skin, followed by the posterior thigh muscles in order to isolate the targeted nerve.

DRG extraction was performed based on my analysis of the protocol found in previous literature [45].

4.3. Immunoblotting

Total 4E-BP2 immunoblotting was performed on the following five organs extracted via dissection from 2-month-old Wild-type male mice: the retinal ganglia, the optic nerve, the dorsal root ganglia, the sciatic nerve, and the whole brain. The immunoblotting process was conducted as described in previous literature [33].

The mice were given access to food and water until they reached the required age for dissection. They were in an aseptic, alternating night and day environment in the animal care facility of my lab. Mice were given isoflurane anesthesia before being euthanized in a carbon dioxide chamber. Tissue samples from the optic nerve, the sciatic nerve, the retinal ganglia, the dorsal root ganglia, and the whole brain were collected. Mouse tissue was lysed and homogenized using RIPA buffer (150 mM sodium chloride,1.0% NP-40, 0.5% sodium deoxycholate, 0.1% SDS, 50 mM Tris, pH 8.0) mixed with protease and phosphatase inhibitors. Samples were then centrifuged for 20 minutes at 16 000 rcf at 4°C. Immunoblotting was done using the supernatant after the protein concentration was determined using the Bradford method. 30 µg of protein was mixed with Laemmli sample buffer (50 mM Tris, pH 6.8, 100 mM DTT, 2% SDS, 10% glycerol, 0.1% bromophenol blue). The mixture was heated at 100°C for 5 minutes and then resolved on a polyacrylamide gel. Proteins were transferred using a 0.2 µm nitrocellulose membrane. After transfer, the membrane was blocked at room temperature using 5% milk for 1 hour. The membrane was then incubated overnight at 4°C using a total 4E-BP2 primary antibody in 5% milk. The membrane was washed with TBS-T three times before applying the goat anti-rabbit secondary antibody (Catalog No. A-11012) for one hour at room temperature. Proteins

 doi:10.20944/preprints202410.2493.v2

were covered in ECL western blotting substrate (Catalog No. 32106) twice for 1 minute and then exposed to X-ray films.

5. Conclusion

This work discovered the neurobiological mechanism of deamidation for the first time. This mechanism's key factor is the axon, which causes 4E-BP2 deamidation due to its proteasome-poor environment. This environment increases the 4E-BP2 half-life, making it longer than Asn 99 and Asn 102 deamidation half-lives, thus assuring deamidation.

The mechanism was validated by conducting 4E-BP2 western blots in five different organs, including the optic nerve, the sciatic nerve, and the retinal ganglia, for which the western blots were conducted for the first time. In both the central and peripheral nervous systems, the experimental results confirmed that deamidation is significantly higher in axons than cell-body enriched ganglia.

The content derived from the results in this study is therefore that 4E-BP2 deamidation is caused by the axons and their unique properties (the proteasome environment), thus validating my discovery.

This validated discovery of the link between 4E-BP2 deamidation and axons is of seminal importance because it explains what causes a post-translational modification in the brain of all mammalian species, which has been conserved for over 90 million years and opens the way to curing all neurodegenerative diseases, such as Alzheimer's, Parkinson's and many others.

This finding allowed me to discover what causes 4E-BP2 to be enriched in the brain compared to other 4E-BP-type proteins. This finding also allowed me to discover and prepare a new and effective treatment for memory loss. Both subsequent findings are on the verge of publication.

My finding revolutionizes humanity's understanding of protein production in the human body. Figure 5 shows a flow sheet describing protein production in mammalian organisms; DNA contains the genetic information carried by messenger RNA (mRNA). eIF4E then binds to the 5′ mRNA cap structure, leading to the ribosome's recruitment. The ribosome then produces proteins. 4E-BP proteins inhibit overall protein production by binding to eIF4E.

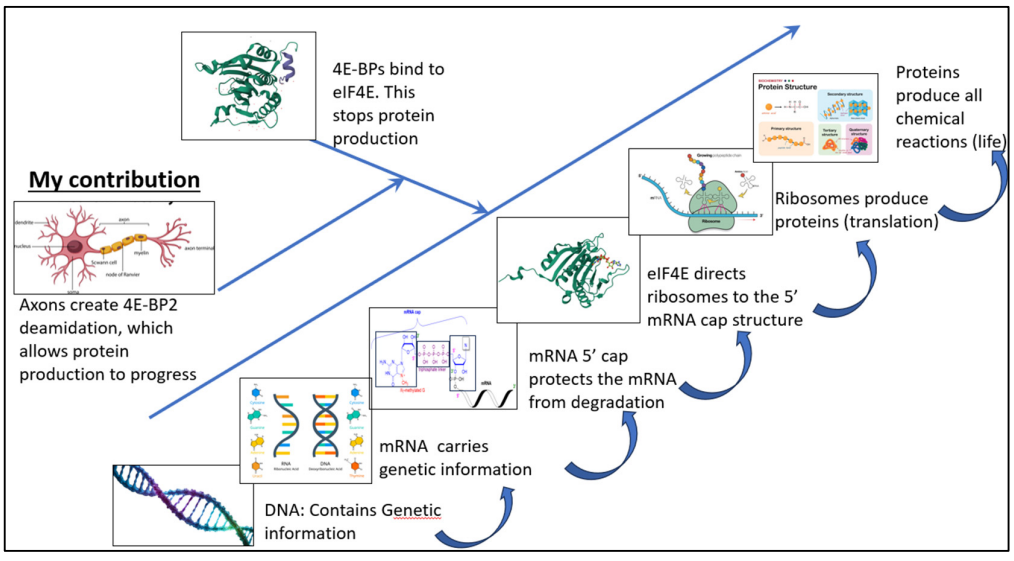

Figure 5. Flow sheet of the impact of the axon on protein production in the mammalian organism.

My contribution fundamentally changes our understanding of translational regulation by demonstrating that the axon is a translational regulator in itself. The axon causes deamidation in the 4E-BP2 protein and, by doing so, stops 4E-BP2 from inhibiting protein production in the nervous system.

 doi:10.20944/preprints202410.2493.v2

Author Contributions: Conceptualization; methodology, experimental validation, formal analysis, investigation, resources, data curation, writing—original draft preparation, writing—review and editing, visualization, supervision, project administration, funding acquisition, DJ. The author has read and agreed to the published version of the manuscript.

Funding: This research received external funding from FLOGEN Technologies Inc.

Conflicts of Interest: Davis Joseph was employed by Flogen Technologies Inc. The author declares that the research was conducted in the absence of any commercial or financial relationships that could be construed as a potential conflict of interest. The authors declare that this study received funding from Flogen Technologies Inc. The funder was not involved in the study design, collection, analysis, interpretation of data, the writing of this article, or the decision to submit it for publication.

References

1. Filipowicz W, Furuichi Y, Sierra JM, Muthukrishnan S, Shatkin AJ, Ochoa S. A protein binding the methylated 5′-terminal sequence, m7GpppN, of eukaryotic messenger RNA. Proceedings of the National Academy of Sciences of the United States of America. 1976;73:1559–1563.
2. Lin TA, Kong X, Haystead TA, Pause A, Belsham G, Sonenberg N, Lawrence JC Jr. PHAS-I as a link between mitogen-activated protein kinase and translation initiation. Science. 1994 Oct 28;266(5185):653-6. doi: 10.1126/science.7939721. PMID: 7939721.
3. Watanabe, A., Takio, K., & Ihara, Y. (1999). Deamidation and Isoaspartate Formation in Smeared Tau in Paired Helical Filaments: Unusual Properties of The Microtubule-Binding Domain Of Tau. Journal of Biological Chemistry, 274(11), 7368-7378. https://doi.org/10.1074/jbc.274.11.7368
4. Shimizu T, Matsuoka Y, Shirasawa T, Biological Significance of Isoaspartate and Its Repair System, Biological and Pharmaceutical Bulletin, (2005), Volume 28, Issue 9, 1590-1596, Released on J-STAGE September 01, 2005, Online ISSN 1347-5215, Print ISSN 0918-6158, https://doi.org/10.1248/bpb.28.1590,
5. Reisz, J. A., Nemkov, T., Dzieciatkowska, M., Culp-Hill, R., Stefanoni, D., Hill, R. C., Yoshida, T., Dunham, A., Kanias, T., Dumont, L. J., Busch, M., Eisenmesser, E. Z., Zimring, J. C., & Hansen, K. C. (2018). Methylation of protein aspartates and deamidated asparagines as a function of blood bank storage and oxidative stress in human red blood cells. Transfusion, 58(12), 2978. https://doi.org/10.1111/trf.14936
6. Bidinosti M, Ran I, Sanchez-Carbente MR, Martineau Y, Gingras AC, Gkogkas C, Raught B, Bramham CR, Sossin WS, Costa-Mattioli M, DesGroseillers L, Lacaille JC, Sonenberg N. Postnatal deamidation of 4E-BP2 in brain enhances its association with raptor and alters kinetics of excitatory synaptic transmission. Mol Cell. 2010 Mar 26;37(6):797-808. doi: 10.1016/j.molcel.2010.02.022. PMID: 20347422; PMCID: PMC2861547.
7. Truong, R. Identifying the mechanism underlying tissue-specific Deamidation of Translation Repressor 4E-BP2, 32 (McGill University, 2017)
8. Nedergaard, M., Kraig, RP, Tanabe, J., & Pulsinelli, WA. (1991). Dynamics of interstitial and intracellular pH in evolving brain infarct. American Journal of Physiology-Regulatory, Integrative and Comparative Physiology. https://doi.org/10.1152/ajpregu.1991.260.3.R581
9. Jessica L. Banko, Francis Poulin, Lingfei Hou, Christine T. DeMaria, Nahum Sonenberg, Eric Klann. The Translation Repressor 4E-BP2 Is Critical for eIF4F Complex Formation, Synaptic Plasticity, and Memory in the Hippocampus, Journal of Neuroscience 19 October 2005, 25 (42) 9581-9590; DOI: 10.1523/JNEUROSCI.2423-05.2005
10. Gkogkas, C., Khoutorsky, A., Ran, I. et al. Autism-related deficits via dysregulated eIF4E-dependent translational control. Nature 493, 371–377 (2013). https://doi.org/10.1038/nature11628
11. Dunkelberger EB, Buchanan LE, Marek P, Cao P, Raleigh DP, Zanni MT. Deamidation accelerates amyloid formation and alters amylin fiber structure. J Am Chem Soc. 2012 Aug 1;134(30):12658-67. doi: 10.1021/ja3039486. Epub 2012 Jul 17. PMID: 22734583; PMCID: PMC3410046.
12. Sharma, V., Sood, R., Lou, D., Hung, T., Lévesque, M., Han, Y., Levett, J. Y., Wang, P., Murthy, S., Tansley, S., Wang, S., Siddiqui, N., Tahmasebi, S., Rosenblum, K., Avoli, M., Lacaille, J., Sonenberg, N., & Khoutorsky, A. (2021). 4E-BP2–dependent translation in parvalbumin neurons controls epileptic seizure threshold. Proceedings of the National Academy of Sciences, 118(15), e2025522118. https://doi.org/10.1073/pnas.2025522118
13. McNamara, NB, Munro, DAD, Bestard-Cuche, N. et al. Microglia regulate central nervous system myelin growth and integrity. Nature 613, 120–129 (2023). https://doi.org/10.1038/s41586-022-05534-y
14. London, A., Benhar, I. & Schwartz, M. The retina as a window to the brain—from eye research to CNS disorders. Nat Rev Neurol 9, 44–53 (2013). https://doi.org/10.1038/nrneurol.2012.227
15. London A, Benhar I, Schwartz M. The retina as a window to the brain-from eye research to CNS disorders. Nat Rev Neurol. 2013 Jan;9(1):44-53. doi: 10.1038/nrneurol.2012.227. Epub 2012 Nov 20. PMID: 23165340.
16. Butt, A., Pugh, M., Hubbard, P. et al. Functions of optic nerve glia: axoglial signalling in physiology and pathology. Eye 18, 1110–1121 (2004). https://doi.org/10.1038/sj.eye.6701595

17. Akobeng AK. Understanding type I and type II errors, statistical power and sample size. Acta Paediatr. 2016 Jun;105(6):605-9. doi: 10.1111/apa.13384. Epub 2016 Mar 31. PMID: 26935977.
18. Prakash, Bhardwaj AK, Devi MN, Sridevi NS, Rao PK, Singh G. Sciatic nerve division: a cadaver study in the Indian population and review of the literature. Singapore Med J. 2010 Sep;51(9):721-3. PMID: 20938613.
19. De Lima, S., Koriyama, Y., Kurimoto, T., Oliveira, J. T., Yin, Y., Li, Y., Gilbert, H., Fagiolini, M., Martinez, A. M., & Benowitz, L. (2012). Full-length axon regeneration in the adult mouse optic nerve and partial recovery of simple visual behaviors. Proceedings of the National Academy of Sciences, 109(23), 9149-9154. https://doi.org/10.1073/pnas.1119449109
20. Bala U, Tan KL, Ling KH, Cheah PS. Harvesting the maximum length of sciatic nerve from adult mice: a step-by-step approach. BMC Res Notes. 2014 Oct 10;7:714. doi: 10.1186/1756-0500-7-714. PMID: 25304607; PMCID: PMC4197312.
21. Mayoral, SR., Etxeberria, A., Shen, AA, & Chan, JR. (2018). Initiation of CNS Myelination in the Optic Nerve Is Dependent on Axon Caliber. Cell Reports, 25(3), 544. https://doi.org/10.1016/j.celrep.2018.09.052
22. Schmalbruch, H. (1986). Fiber composition of the rat sciatic nerve. The Anatomical Record, 215(1), 71-81. https://doi.org/10.1002/ar.1092150111
23. Saliani, A., Perraud, B., Duval, T., Stikov, N., & Rossignol, S. (2017). Axon and Myelin Morphology in Animal and Human Spinal Cord. Frontiers in Neuroanatomy, 11, 300929. https://doi.org/10.3389/fnana.2017.00129
24. Stassart, R. M., Möbius, W., Nave, A., & Edgar, J. M. (2018). The Axon-Myelin Unit in Development and Degenerative Disease. Frontiers in Neuroscience, 12. https://doi.org/10.3389/fnins.2018.00467
25. Yadav, D., Lee, J. Y., Puranik, N., Chauhan, P. S., Chavda, V., Jin, O., & W. Lee, P. C. (2022). Modulating the Ubiquitin–Proteasome System: A Therapeutic Strategy for Autoimmune Diseases. Cells, 11(7). https://doi.org/10.3390/cells11071093
26. Shi Y, Rhodes NR, Abdolvahabi A, Kohn T, Cook NP, Marti AA, Shaw BF. Deamidation of asparagine to aspartate destabilizes Cu, Zn superoxide dismutase, accelerates fibrillization, and mirrors ALS-linked mutations. J Am Chem Soc. 2013 Oct 23;135(42):15897-908. doi: 10.1021/ja407801x. Epub 2013 Oct 10. PMID: 24066782.
27. Robinson NE, Robinson AB. Deamidation of human proteins. Proc Natl Acad Sci U S A. 2001 Oct 23;98(22):12409-13. doi: 10.1073/pnas.221463198. Epub 2001 Oct 16. PMID: 11606750; PMCID: PMC60067.
28. Robinson NE, Robinson AB. Molecular clocks. Proc Natl Acad Sci U S A. 2001 Jan 30;98(3):944-9. doi: 10.1073/pnas.98.3.944. PMID: 11158575; PMCID: PMC14689.
29. Dawson, J.E., Bah, A., Zhang, Z. et al. Non-cooperative 4E-BP2 folding with exchange between eIF4E-binding and binding-incompatible states tunes cap-dependent translation inhibition. Nat Commun 11, 3146 (2020). https://doi.org/10.1038/s41467-020-16783-8
30. Borchelt DR, Ratovitski T, van Lare J, Lee MK, Gonzales V, Jenkins NA, Copeland NG, Price DL, Sisodia SS. Accelerated amyloid deposition in the brains of transgenic mice coexpressing mutant presenilin 1 and amyloid precursor proteins. Neuron. 1997 Oct;19(4):939-45. doi: 10.1016/s0896-6273(00)80974-5. PMID: 9354339.
31. Valentine JS, Doucette PA, Potter SZ. Copper-Zinc Superoxide Dismutase and Amyotrophic Lateral Sclerosis J Annual Review of Biochemistry, Volume 74, 2005, 563-593, https://doi.org/10.1146/annurev.biochem.72.121801.161647
32. Yamaguchi M, Kubo M, Fukuda H, Demura T. Vascular-related NAC-DOMAIN7 is involved in the differentiation of all types of xylem vessels in Arabidopsis roots and shoots. Plant J. 2008 Aug;55(4):652-64. doi: 10.1111/j.1365-313X.2008.03533.x. Epub 2008 Apr 24. PMID: 18445131.
33. Kouloulia S, Hallin EI, Simbriger K, Amorim IS, Lach G, Amvrosiadis T, Chalkiadaki K, Kampaite A, Truong VT, Hooshmandi M, Jafarnejad SM, Skehel P, Kursula P, Khoutorsky A, Gkogkas CG. Raptor-Mediated Proteasomal Degradation of Deamidated 4E-BP2 Regulates Postnatal Neuronal Translation and NF-κB Activity. Cell Rep. 2019 Dec 10;29(11):3620-3635.e7. doi: 10.1016/j.celrep.2019.11.023. PMID: 31825840; PMCID: PMC6915327.
34. Rolfs, Z., Frey, BL., Shi, X. et al. An atlas of protein turnover rates in mouse tissues. Nat Commun 12, 6778 (2021). https://doi.org/10.1038/s41467-021-26842-3
35. Fusco, C.M., Desch, K., Dörrbaum, A.R. et al. Neuronal ribosomes exhibit dynamic and context-dependent exchange of ribosomal proteins. Nat Commun 12, 6127 (2021). https://doi.org/10.1038/s41467-021-26365-x
36. Cheng HC, Ulane CM, Burke RE. Clinical progression in Parkinson disease and the neurobiology of axons. Ann Neurol. 2010 Jun;67(6):715-25. doi: 10.1002/ana.21995. PMID: 20517933; PMCID: PMC2918373.
37. Nishimune, H., & Shigemoto, K. (2018). Practical anatomy of the neuromuscular junction in health and disease. Neurologic Clinics, 36(2), 231. https://doi.org/10.1016/j.ncl.2018.01.009
38. MacDougall, J. D., Sale, D. G., Alway, S. E., & Sutton, J. R. (1984). Muscle fiber number in biceps brachii in bodybuilders and control subjects. Journal of Applied Physiology. https://doi.org/10.1152/jappl.1984.57.5.1399

39. Nishimune, H., & Shigemoto, K. (2018). Practical anatomy of the neuromuscular junction in health and disease. Neurologic Clinics, 36(2), 231. https://doi.org/10.1016/j.ncl.2018.01.009
40. Leeuwin RS, Wolters EC. Effect of corticosteroids on sciatic nerve-tibialis anterior muscle of rats treated with hemicholinium-3. An experimental approach to a possible mechanism of action of corticosteroids in myasthenia gravis. Neurology. 1977 Feb;27(2):171-7. doi: 10.1212/wnl.27.2.171. PMID: 189257.
41. Colasante C, Brouard MO, Pécot-Dechavassine M. Synaptophysin (p38) immunolabelling at the mouse neuromuscular junction. Neuromuscul Disord. 1993 Sep-Nov;3(5-6):395-400. doi: 10.1016/0960-8966(93)90084-w. PMID: 8186682.
42. Krause Neto W, Gama EF, Silva WA, de Oliveira TVA, Vilas Boas AEDS, Ciena AP, Anaruma CA, Caperuto ÉC. The sciatic and radial nerves seem to adapt similarly to different ladder-based resistance training protocols. Exp Brain Res. 2022 Mar;240(3):887-896. doi: 10.1007/s00221-021-06295-2. Epub 2022 Jan 25. PMID: 35075497.
43. Rashidiani-Rashidabadi, A., Heidari, M. H., Sajadi, E., Hejazi, F., Fathabady, F. F., Sadeghi, Y., Aliaghaei, A., Raoofi, A., Abdollahifar, A., & Farahni, R. M. (2019). Sciatic nerve injury alters the spatial arrangement of neurons and glial cells in the anterior horn of the spinal cord. Neural Regeneration Research, 14(10), 1833-1840. https://doi.org/10.4103/1673-5374.257539
44. Livingston, A. Microtubules in myelinated and unmyelinated axons of rat sciatic nerve. Cell Tissue Res. 182, 401–407 (1977). https://doi.org/10.1007/BF00219774
45. Sleigh, J.N., West, S.J. & Schiavo, G. A video protocol for rapid dissection of mouse dorsal root ganglia from defined spinal levels. *BMC Res Notes* **13**, 302 (2020). https://doi.org/10.1186/s13104-020-05147-6